

## Vortex dynamics under selective rotating-wall excitation of Kelvin-Helmholtz waves in a nonneutral plasma

G. Maero<sup>1,2</sup>, N. Panzeri<sup>1,2</sup>, R. Pozzoli<sup>1</sup>, M. Romé<sup>1,2</sup>

<sup>1</sup> Dipartimento di Fisica, Università degli Studi di Milano, Italy

<sup>2</sup> INFN Sezione di Milano, Italy

Penning-Malmberg (magneto-electrostatic) traps are an excellent environment to investigate the nonlinear dynamics of collective systems like two-dimensional (2D) inviscid fluids, due to the analogy between such systems and trapped single-component plasmas. In this analogy, the plasma density (which can be considered as uniform along the longitudinal axis of the cylindrically-symmetric confinement volume) is isomorphic to the fluid vorticity and the velocity fields correspond to one another. This has motivated a wealth of nonneutral plasma-based investigations on 2D fluid dynamics [1, 2, 3, 4, 5]. On the other way round, the understanding and control of fluid-like perturbations and instabilities is of paramount importance in nonneutral plasmas used, e.g., in antimatter synthesis and confinement [6, 7]. A class of perturbations of long-standing interest in this context is that of the so-called diocotron modes, i.e. Kelvin-Helmholtz (KH) density waves travelling in the polar direction  $\theta$ , expanded in normal (Fourier) modes  $l$ . In the case of a single, initially circular vortex the  $l$ -th KH mode can be seen as a rotating multipolar deformation of order  $l$  of the circular profile.

Producing a  $\theta$ -asymmetric vortex with a specific mode  $l$  and arbitrary amplitude may be technically difficult, as the straightforward way would be to apply an  $l$ -polar electric field to the trap boundary at the mode resonant frequency  $\omega_l$ , thus requiring to split a trap electrode in  $2l$  polar patches - and typical segmentation is up to 4 or 8 segments only. We have circumvented this limitation with a technique based on tailored multipolar rotating fields applied to a 4- or 8-segmented electrode. The selection of the field multipole (dipole to quadrupole (octupole), for 4-fold (8-fold) split electrode), rotation direction and frequency leads to the ‘clean’ excitation of the single, selected mode of arbitrary wavenumber, starting from an initial state consisting in a single, axisymmetric column of an electron plasma [8]. In a series of experiments we analyzed the dynamics and final states attained by the application of this technique.

The experimental routine starts with the generation of an electron plasma by low-power radio-frequency ionization of the background gas (pressure  $\leq 10^{-8}$  mbar), which produces a vortex revolving around the trap axis (i.e. a pronounced  $l = 1$  KH mode) [9, 10]; feedback damping allows the plasma column to be brought onto the trap axis and thermalize to a quasi-uniform density circular vortex in rotational equilibrium at rotation frequency  $\omega_{rot} = ne/2\epsilon_0 B$  (tens of

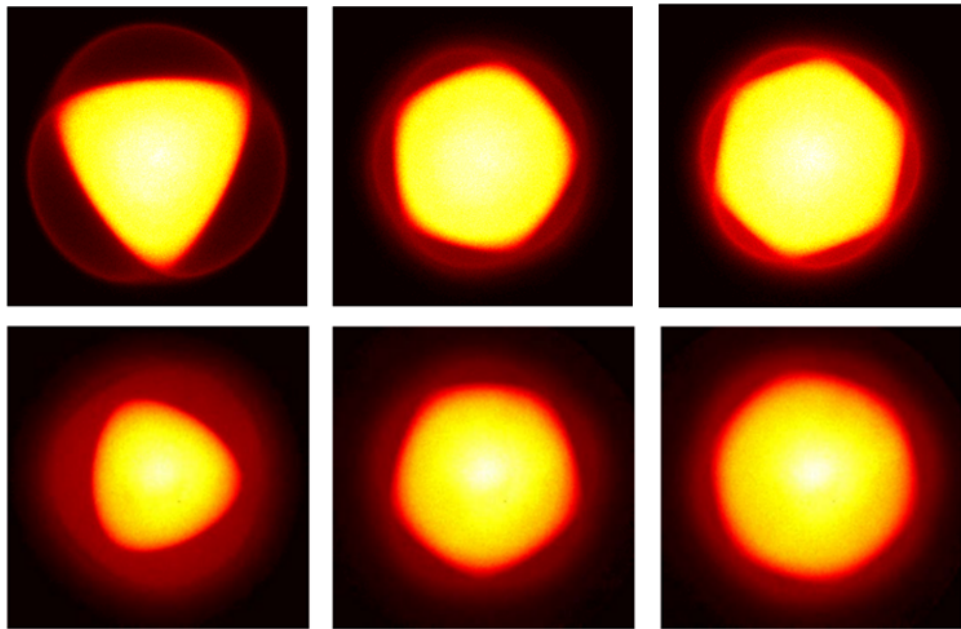


Figure 1: Selective excitation of single KH waves. Top row: Modes 3, 5 and 6 at saturation after  $\sim 10^2 \tau_{rot}$ . Bottom row: The same modes after a long excitation ( $\geq 10^3 \tau_{rot}$ ).

kHz, with typical densities  $n \sim 10^{12} - 10^{13} \text{ m}^{-3}$  and magnetic field strengths  $B \sim 0.1 - 0.2 \text{ T}$ ); finally, the excitation field is applied for the desired amount of time. The plasma is released from the confinement and flows longitudinally onto a biased phosphor screen, where an image of the axially-integrated density is formed. Low-order modes ( $l \leq 3$ ) can be non-destructively monitored using the electrostatic signals induced by the KH waves on suitable segmented electrodes.

Figure 1 shows some examples of modes brought to large amplitude (nonlinear regime) starting from the axisymmetric initial state, using different rotating fields at the respective resonant frequencies. Resonances were experimentally determined via systematic repetition of the excitation sequence in a broad frequency range. Within some tens of vortex rotation periods  $\tau_{rot}$  the dominant modes reach their saturation amplitude, where filamentation from the nonlinear deformations and ‘cat’s eye’ structures appear (top row). If the excitation continues, over much longer times (several  $10^2$  to  $\sim 10^3 \tau_{rot}$ ) one can still observe a deformed state, albeit in a much more prominent background formed by the mixing of filamented plasma (bottom row). Resonance curves (not shown here) undergo significant broadening and stronger drives may be required, although always in a fairly weak perturbation regime (drive amplitude  $\ll$  plasma potential).

We can get further insight from the electrostatic signals. Figure 2 shows the example of an  $l = 3$  mode excited by a dipole field applied on a 4-fold split electrode and rotation in the opposite direction with respect to plasma rotation, at the resonant frequency of 54 kHz. The  $l = 3$

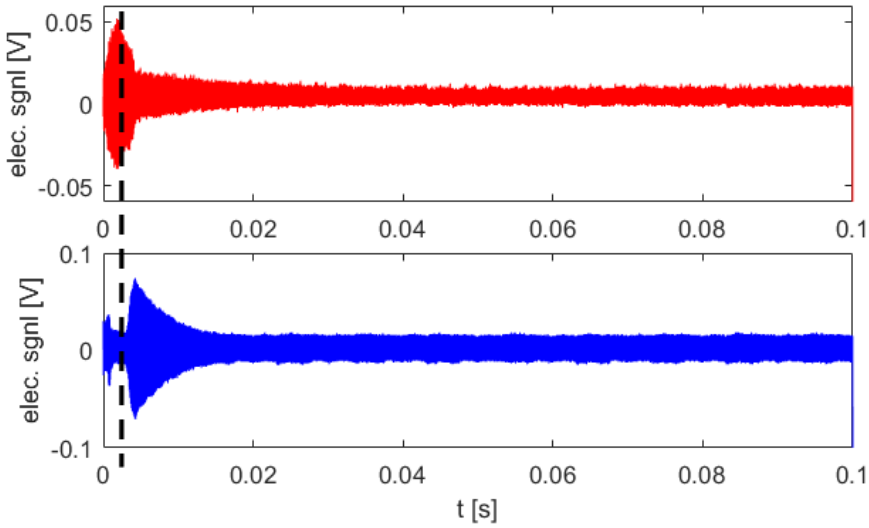


Figure 2: Electrostatic signals induced by the KH waves on segmented trap electrodes during the rotating-field excitation at resonant frequency. Top:  $l = 3$  signal. Bottom:  $l = 2$  signal. The dashed line indicates the time corresponding to  $l = 3$  saturation.

mode signal (top row) rapidly grows to saturation and undergoes a catastrophic collapse within  $\sim 2$  ms (some ten  $\tau_{rot}$ ). The collapse is accompanied by a sudden growth of the adjacent lower mode  $l = 2$ , later also damped (bottom row). These features elucidate how once the mode has reached a high amplitude, a strong mode damping occurs through the formation of filamentation and build-up of low-density background, where the vortex tries to recover the axisymmetric equilibrium state through a mode cascade. Yet if the final state is not too dissimilar with respect to the initial one, it can couple again to the drive and the dominant mode is recovered. In some cases we have observed multiple stages of recoupling and damping (not shown here).

The precise control of the deformed vortex state is affected by features such as the very fast mode growth and the inherent repeatability limitations (e.g., shot-to-shot variations of the plasma density profile). These can be effectively counteracted by adapting the excitation technique from a set-frequency to a swept-frequency (autoresonant) drive, exploiting the relation between mode frequency and amplitude to lock the mode to the external forcing and control the growth [11]. Preliminary results are shown in Fig. 3: Here the same initial state as in Fig. 2 is subjected to a drive with a 100 ms linear frequency sweep from 66 to 52 kHz. The  $l = 3$  mode (top row) growth is slower by almost an order of magnitude (hence easier to adjust to obtain the desired amplitude). Once a highly-deformed state is reached,  $l = 3$  damping and collapse to the lower mode occur again. One may notice that mode-drive coupling occurs well before the actual resonant frequency (54 kHz, reached around 85 ms), a feature possibly explained, at

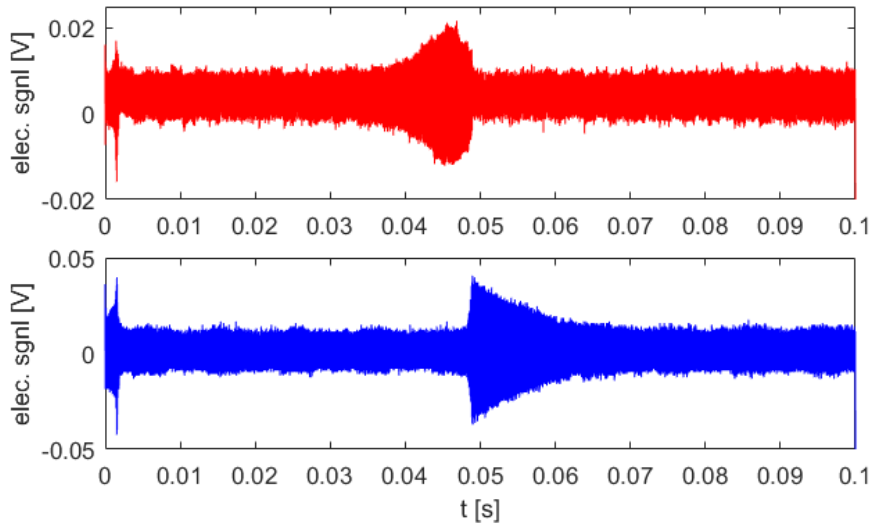


Figure 3: Electrostatic signals induced by the KH waves on segmented trap electrodes during the downward swept-frequency rotating-field excitation. Top:  $l = 3$  signal. Bottom:  $l = 2$  signal.

least partially, by the natural resonance width, yet contrasting with known instances of autoresonant excitation. Particle-In-Cell simulations using a tailored code [12] have been performed to support the experimental results, qualitatively confirming all the details of the forced evolution. Again, while autoresonant features are apparent (e.g., mode growth is qualitatively the same above a certain drive amplitude threshold), early coupling to the drive appears. Further systematic investigation of these aspects is ongoing, both via experiments and simulations, with a special attention to plasma parameters such as the radial density profile and, in perspective, to the evolution and stability of vortices after the excitation is interrupted.

## References

- [1] C. F. Driscoll and K. S. Fine, *Phys. Fluids B* **2**, 1359 (1990)
- [2] T. B. Mitchell and C. F. Driscoll, *Phys. Rev. Lett.* **73**, 2196 (1994)
- [3] F. Lepreti, M. Romé, G. Maero, B. Paroli, R. Pozzoli and V. Carbone, *Phys. Rev. E* **87**, 063110 (2013)
- [4] S. Chen, G. Maero and M. Romé, *J. Plasma Phys.* **81**, 495810511 (2015)
- [5] N. C. Hurst, J. R. Danielson, D. H. E. Dubin and C. M. Surko, *Phys. Plasmas* **27**, 042101 (2020)
- [6] J. R. Danielson, D. H. E. Dubin, R. G. Greaves and C. M. Surko, *Rev. Mod. Phys.* **87**, 247 (2015)
- [7] J. Fajans and C. M. Surko, *Phys. Plasmas* **27**, 030601 (2020)
- [8] M. Romé, G. Maero, N. Panzeri and R. Pozzoli, 46th EPS Conf. on Plasma Phys., ECA **43C**, P2.4003 (2019)
- [9] G. Maero, S. Chen, R. Pozzoli and M. Romé, *J. Plasma Phys.* **81**, 495810503 (2015)
- [10] G. Maero, *Il Nuovo Cimento C* **40**, 90 (2017)
- [11] J. Fajans, E. Gilson and L. Friedland, *Phys. Rev. Lett.* **82**, 4444 (1999)
- [12] G. Maero, M. Romé, F. Lepreti and M. Cavenago, *Eur. Phys. J. D* **68**, 277 (2014)